Applied Nanoscience (2022) 12:2195–2205
https://doi.org/10.1007/s13204-022-02474-x

ORIGINAL ARTICLE

The study of TiO_2/Cu_2O nanoparticles as an efficient nanophotocalyst toward surface adsorption and photocatalytic degradation of methylene blue

Mona Hosseini-Sarvari[1] · Fattaneh Jafari[1] · Abdulhamid Dehghani[1]

Received: 7 February 2022 / Accepted: 24 March 2022 / Published online: 18 April 2022

Abstract
Herein, cost-effective TiO_2/Cu_2O nanoparticles were synthesized via a simple reaction route and applied-for efficient photodegradation of methylene blue (MB) as a model organic dye. Due to the high surface area of TiO_2/Cu_2O nanoparticles, adsorption and photodegradation properties were evaluated toward MB degradation, showing a high adsorption yield of about 95.7% along with a 100.0% photodegradation efficiency. The effective factors on both adsorption and photodegradation process including pH, initial concertation of organic dye, amount of TiO_2/Cu_2O nanoparticles, and temperature were optimized via the one-factor-at-a-time optimization method. The photocatalytic performances of TiO_2/Cu_2O nanoparticles were compared with the activity of both Degussa p25 TiO_2 and Cu_2O nanoparticles, showing very higher adsorption and photodegradation yields toward dye degradation. It should be noted that the mechanism of the photodegradation of MB on the surface of TiO_2/Cu_2O nanoparticles was investigated, revealing an adsorption/photodegradation reaction pathway for this phenomenon.

Keywords Photocatalysis · Photodegradation · TiO_2/Cu_2O · Dyes · Methylene blue (MB) · Water purification

Introduction

Nowadays, colored wastewater can be introduced as an enduring challenge for the environment and humanity. The origin of these effluents can be traced to various industries including textile, dyeing, plastic, paper, food, and cosmetics industries(Cao et al. 2017; Slokar and Marechal 1998; Zou et al. 2016; Forgacs et al. 2004; Xu et al. 2019; Ghafoor et al. 2017). In the nineteenth century, with the discovery of the first artificial dye by William Henry, a great revolution took place in the paint industry, including artificial dye, and finally, at the end of the nineteenth century, more than 10,000 artificial dyes were produced. These products were considered a favorable factor for water pollution and the ecosystems of living organisms. In today's world, the textile industry has the most use of dyes. Since the structure of dyes is stable in terms of chemical and photolytic parameters as well as complex aromatic structure, it remains unchanged in some decomposition processes, including biological processes. Therefore, it can be said that it is usually difficult to destroy these paints, so the complexity and toxicity of wastewater components can be attributed to this, although in recent years, various methods such as ozonation, filtration, electrolysis have been used, most of these methods have been less used due to toxic intermediates, high costs, and interference of other components in the wastewater(Kuriechen et al. 2011; Şengil and Özacar 2009; Almeida et al. 2009; Özer and Dursun 2007; Wang and Yang 2016; Yang and Qiu 2010; Ahmed et al. 2017; Zaied and Bellakhal 2009).

It should not be forgotten that human beings have used dyes in various industries for thousands of years, and unfortunately today, more than one and a half million tons of dyes are produced annually, of which 10–15% of the initial volume enters the natural cycle as wastewater. Therefore, it can be said that wastewater treatment can be introduced as one of the most difficult cases of treatment. Therefore, the study of removal and decolorization has become an important topic for researchers in recent years, and finally, many articles in the field of dye removal have been published (Gupta 2009; Ahmad et al. 2009, 2011, 2012). Textile effluents make up

✉ Mona Hosseini-Sarvari
hossaini@shirazu.ac.ir

[1] Nano Photocatalysis Lab, Department of Chemistry, Shiraz University, 7194684795 Shiraz, I.R., Iran

about 17–20% of water pollution, which must be treated or reduced to low-risk secondary pollution due to hazardous environmental effects. Because these pollutants can reduce the oxygen content of water, reduce photosynthesis due to lack of sunlight, reduce quality and also change the color of the water. Therefore, today, the treatment of textile dyes and effluents from textile dyes has become one of the most challenging issues, and various methods have been used to treat dyes, including chemical, physical and biological methods, each of which these methods have its advantages and disadvantages (Lucas and Peres 2007; Hong et al. 2013; Aksu 2005; Somasiri et al. 2008).

Dyes can be classified based on various parameters such as dissolution (solution and Insoluble), bond type, chemical properties, functional groups, ionic charge classification isolated in solution. Dyes can be introduced into two general categories of ionic and non-ionic dyes. Ionic dyes can be divided into two categories: cationic (base) and anionic dyes (direct; acidic; reactive), each of which has its characteristics, application, as well as its unique toxicity. Cationic dyes in the paper industry and modified nylons are used, and one of the most well-known cationic dyes is methylene blue (MB). Due to its aromatic nature, this compound is often toxic, carcinogenic, mutagenic, and is introduced as a biodegradable compound. Therefore, effluents of this color are very dangerous for the ecosystem and the environment and can cause damage such as burning sensation, vomiting, increased heart rate, tissue necrosis, gout, and methemoglobinemia in humans (Ponnusami et al. 2008; Ding et al. 2016; Saeed et al. 2009; Aravind et al. 2021; Mashkoor and Nasar 2020; Eltaweil et al. 2020; Rahimian and Zarinabadi 2020; Santoso et al. 2020).

In recent years, the use of semiconductors such as TiO_2, ZnO, ZrO_2, and WO_3 in water treatment through photocatalytic oxidation processes by ultraviolet radiation due to the high efficiency of this process compared to other methods, has been paid much attention. Photocatalytic processes are often based on the production of highly active species such as hydroxyl radicals, which rapidly oxidize a wide range of organic pollutants (Li et al. 2020a; Chen et al. 2020; Wei et al. 2020; He et al. 2020; Akpan and Hameed 2009; Muruganandham and Swaminathan 2004; Mohabansi et al. 2011; Lin et al. 2012).

Among semiconductors, TiO_2 due to its low cost, nontoxicity, high chemical stability, availability, and high efficiency as an efficient photocatalyst in the field of water treatment for oxidation of organic compounds, detoxification, reduction of toxic metals, effective removal of heavy metals, and bacterial removal is used (Khasawneh and Palaniandy 2020; Lee and Li 2021; Onwuka et al. 2021; Li et al. 2020b). It should be noted that this photocatalyst, in addition to removing contaminants, is also used to remove the color and taste of water (Xiong et al. 2010; Messih et al. 2017; Hosseini-Sarvari and Hosseinpour 2019; Joshi and Shrivastava 2011). But the disadvantages of this metal oxide are the lack of visible light absorption, low quantum efficiency than visible light, high band fission, and rapid recombination of the electron/hole pair (e^-/h^+). In other words, titanium dioxide is a photocatalyst with a bandwidth of 3.2 eV, which is activated only by ultraviolet rays, and it should be noted that only 4% of sunlight contains ultraviolet light (Hosseini-Sarvari et al. 2018a; Hosseini-Sarvari and Dehghani 2020; Linsebigler et al. 1995; Fagan et al. 2016). Therefore, the use of titanium dioxide as a photocatalyst is justified when, given the costs of ultraviolet light and its dangers, we seek to design and modify titanium dioxide that can operate in visible light or even sunlight. In recent years, researchers have devoted much research to the development of effective photocatalyst-based methods for this photocatalyst. One of these methods is hetero-junctions with other materials, especially p-type Cu_2O semiconductors. Cu_2O as a photocatalyst with a 2 eV fission band can absorb visible light and can produce electron holes and transfer the produced electrons to CB TiO_2, so in this system, CB TiO_2 electrons can be reduced and VB Cu_2O holes can be oxidized (Wang et al. 2013; Zheng et al. 2009; Jongh et al. 1999; Hosseini-Sarvari et al. 2018b; Yang et al. 2010; Tavakolian et al. 2021; Li et al. 2015, 2019; Aguirre et al. 2017; Muscetta et al. 2020; Zhang et al. 2013). As a result, this semiconductor composite can be used as an efficient photocatalyst in photocatalytic systems. Due to the necessities expressed in this research, the removal of methylene blue as a dye pollutant for the environment was investigated by the TiO_2/Cu_2O photocatalytic process using visible light. In recent years, this catalyst has been synthesized in our research group and its various optical and non-optical applications have been studied and published (Hosseini-Sarvari et al. 2018b; Tavakolian et al. 2021; Hosseini-Sarvari and Jafari 2020).

Experimental section

Preparation of TiO_2/Cu_2O nanoparticles as photocatalyst

Cu_2O/TiO_2 nanocomposites were formed by the modified subsequent method. 13.2 g quantity of cupric acetate monohydrate was dissolved in DI water (600 mL). Then, 3.2 mL polyethylene glycol 300 (PEG 300) was added to the above solution under vigorous stirring. Subsequently, 0.7 g of tetrabutyl titanate dissolved in ethanol (2–3 mL) and was added to the solution of cupric acetate dropwise. After producing a white precipitate, 15 mL hydrazine (5 M) and 5 mL NaOH (5 M) were added dropwise to the solution under stirring at ambient temperature. After completion of the reaction, the resulted orange precipitates were collected

by centrifuge at 4000 rpm for 5 min and washed with Di-water for neutralization and further washed with acetone (three times). Finally, the powder was dried at 200 °C for 3 h in an oven and then remained at 40 °C for 24 h in a vacuum oven (Han et al. 2009).

Photocatalytic activity of TiO_2/Cu_2O nanoparticles

To investigate the photocatalytic activity of TiO_2/Cu_2O nanoparticles as the photocatalyst, the degradation of methylene blue(MB) was performed under both light and dark conditions. To do this, initially, 10 mg of the photocatalyst was added to 15.0 mL DI water, followed by 30.0 min sonication under dark conditions. Afterward, 15.0 mL MB (5×10^{-5} M) aqueous solution was introduced to the above mixture and the mixture was incubated for 60.0 min in the dark conditions. The UV–Vis spectra of the mixture were recorded by sampling every 30.0 min to probe the variations of dye concertation. Then, the reaction mixture was exposed to daylight for 60.0 min, and to the light fluorescent lamp for another 60.0 min to investigate the photocatalytic activity of the as-prepared TiO_2/Cu_2O nanoparticles via probing the variations of MB concentration by recording the UV–Vis spectra of dye every 30.0 min (λ_{max} of 668 nm). It should be noted that the photocatalyst was separated from the dye solution via several centrifuges and the absorbances were recorded against a reagent blank containing all sample components except MB. It is noteworthy that the photodegradation yield of organic dye was estimated by the following formula:

$$\text{Degradation Efficiency} = \left(C_0 - C\right)/C_0 \times 100,$$

which C_0 and C are represented to the initial and final concentration of MB in the reaction media.

Results and discussion

Optical properties of TiO_2/Cu_2O nanoparticles

To compare to optical properties, the UV–Visible diffuse reflectance spectra of TiO_2, Cu_2O, and TiO_2/Cu_2O NPs are shown in Fig. 1. The absorption edge of TiO_2 nanoparticles is at 386 nm. The redshift of absorption edge from 386 nm for TiO_2 nanoparticles to the higher area for TiO_2/Cu_2O NPs is due to the Cu_2O. The UV–Visible diffuse reflectance spectra results demonstrate that Cu_2O loading shifts the absorption edge of TiO_2 NPs into the visible region, which in turn decreases the bandgap energy. Decreasing the bandgap after the combination of these two metal oxides implies a high level of interaction between Cu_2O and TiO_2 NPs. This suggests that the decoration of Cu_2O with the TiO_2 NPs has a significant impact on the absorption of visible light. The optical band gaps of TiO_2, Cu_2O, and TiO_2/CuO_2 NPs were 3.2, 2.18, and 2.76 eV, respectively, which were determined by $E = h^*C/\lambda_{max}$ (Dharma et al. 2009). Noticeably, the bandgap of the TiO_2/CuO_2 photocatalyst is characteristically lower than the unmodified TiO_2 NPs, and by treatment of TiO_2 NPs with Cu_2O, the bandgap of TiO_2 NPs was significantly reduced, indicating the successful coupling of the Cu_2O in the TiO_2 structure.

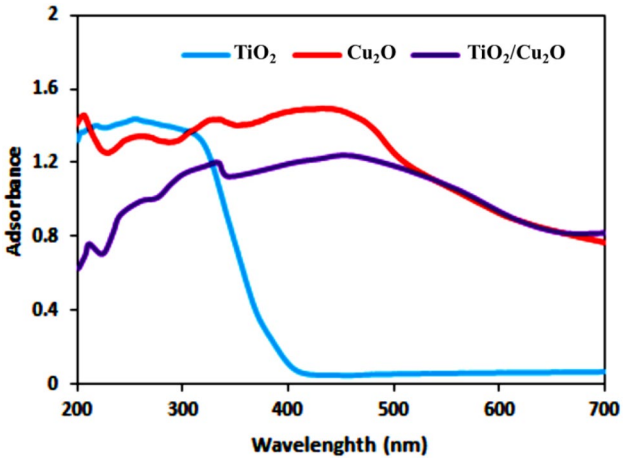

Fig. 1 UV–Vis diffuse reflection absorption spectra of TiO_2, Cu_2O, and TiO_2/Cu_2O nanoparticles

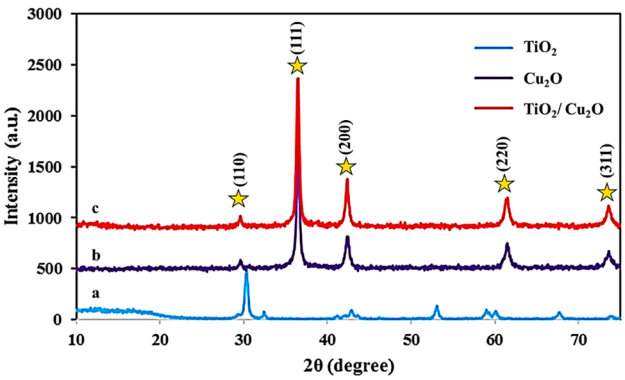

Fig. 2 XRD pattern of the **a** TiO_2, **b** Cu_2O, and **c** TiO_2/Cu_2O nanoparticles photocatalyst

XRD patterns

XRD patterns are shown in Fig. 2 exhibit the crystalline structure of (a) TiO_2, (b) Cu_2O, and (c) TiO_2/Cu_2O nanoparticles. Reflections are observed at $2\theta = 29.87^\circ$, 36.48°, 42.37°, 61.45° and 73.51° belonging to the (110), (111), (200), (220) and (311) crystal planes of Cu_2O, respectively (Reference JCPDS card No. 05-0667) (Liu et al. 2014). For TiO_2/Cu_2O, no diffraction peaks of TiO_2 could be detected, and all diffraction peaks belonged to the Cu_2O phase, which

can be related to factors such as low Ti content or excessive TiO_2 dispersion, which was confirmed by ICP analysis. The Cu_2O loading was confirmed by the inducted coupled plasma analyzer. The amount of Ti and Cu was 6.27% (*w*/*w*) and 30.06% (*w*/*w*), respectively, indicating the successful coupling of the Cu_2O in the structure. In the end, the mean diameter of Cu_2O nanoparticles was calculated using Scherrer's equation to be around 34 nm ($2\theta = 36.48^\circ$, $\lambda = 0.154178$ nm for copper, FWHM = 0.2597, $K = 0.94$).

$$D = K\lambda/\beta\cos\theta \left(\text{Scherrer}'\text{s equation}\right),$$

where λ is the wavelength of X-ray radiation, K is the Scherrer's constant, θ is the Bragg angle, β is the half-width full maximum of the peak.

BET surface area

BET surface area The N_2 adsorption–desorption isotherm of the TiO_2/Cu_2O nanoparticles is presented in Fig. 3. For the prepared TiO_2/Cu_2O, the specific surface area is calculated by the Brunauer – Emmett – Teller (BET) and the Langmuir methods, which are about 32.663 and 39.282 m^2/g, respectively. The total pore volume and mean pore diameter of the prepared TiO_2/Cu_2O are estimated to be 0.091 cc/g and 3.891 nm, respectively (Table1).

To obtain a better view of the photocatalytic performances of TiO_2/Cu_2O nanoparticles, the surface adsorption and photodegradation catalytic activity was first evaluated by degradation of MB (2.5 × 10–5 M, 8 ppm) in an aqueous solution. The UV–Vis absorbance curves of MB in aqueous solution during the degradation process is shown in Fig. 4a. It is noted that MB showed characteristic adsorption at 664 nm, and the intensity gradually decreased along with the illumination time. The corresponding photographs of the samples taken at intervals in Fig. 4b also displayed that the initial MB aqueous solution with blue color turned to be

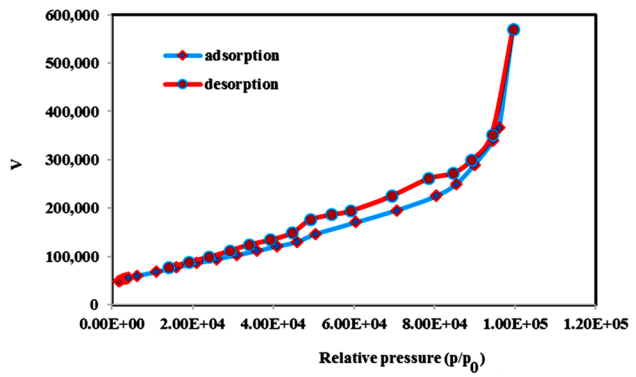

Fig. 3 Nitrogen adsorption – desorption isotherm of TiO_2/Cu_2O nanoparticles

Table 1 Results of BET surface area measurements for TiO_2/Cu_2O nanoparticles

BJH adsorption summary	
Surface area	39.282 m^2/g
Pore volume	0.091 cc/g
Pore diameter Dv(d)	3.891 nm
BJH desorption summary	
Surface area	47.576 m^2/g
Pore volume	0.093 cc/g
Pore diameter Dv(d)	3.766 nm
BET summary	
Surface area	32.663 m^2/g
Total pore volume summary	
Total pore volume = for pores smaller than 51.1 nm (Diameter) at P/Po = 0.96089	$5.668e-02$ cc/g

transparent after 180 min. At first, to ensure complete surface adsorption, a solution of MB in water was mixed with TiO_2/Cu_2O and stirred for 1 h in a dark condition. In dark conditions after 1 min, an obvious change can be seen and the absorbance of MB (2.5×10^{-5} M) was decreased greatly from 0.116 to 0.005 (95.68% decolorization efficiency). According to this, surface adsorption of MB by TiO_2/Cu_2O nanoparticles is very fast at first even in dark conditions. This result shows that TiO_2/Cu_2O nanoparticles have very strong absorbability toward MB so that MB molecules could be transferred from the solution to the surface in a short time in dark conditions.

However, to prove the existence of a boundary between reversible adsorption and irreversible photocatalytic decomposition of MB, the dye desorption process was performed before and upon photo-irradiation tests. To do this, the dye adsorption (8.0 mg/L) was carried out upon optimal conditions at dark conditions, then the dye desorption from the surface of TiO_2/Cu_2O nanoparticles was performed upon the repetitive washings and centrifuges to complete desorption of organic dye from the surface of the TiO_2/Cu_2O nanoparticles. Afterward, the absorbance of the supernatant was recorded and the concentration of desorbed dye was calculated. The results showed that without photo-irradiation, the concentration of desorbed dye in the supernatant was 7.6 mg/L. It means that without photo-irradiation, the organic dye was only adsorbed on the surface of TiO_2/Cu_2O which is a reversible process. Moreover, the dye desorption test was performed for 8.0 mg/L of MB after the photo-irradiation process. The results showed that the dye concentration in the supernatant was about 0.1 mg/L, indicating that 98% of dye was irreversibly decomposed on the surface of TiO_2/Cu_2O upon photo-irradiation. Hence, this experiment proved the existence of a boundary between reversible adsorption and irreversible photocatalytic decomposition using the as-prepared TiO_2/Cu_2O.

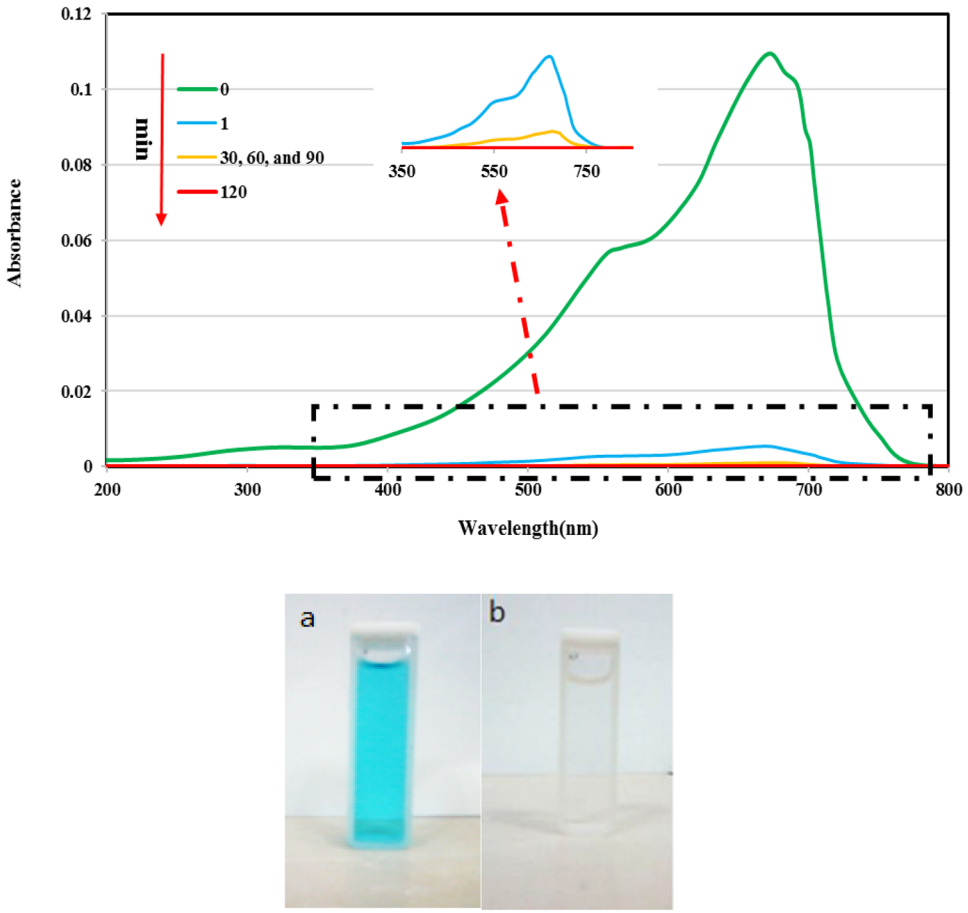

Fig. 4 **a** The absorbance curves of MB in aqueous solution using TiO_2/Cu_2O nanoparticles, **b** The photographs of MB in aqueous solution before and after surface adsorption and photodegradation

To provide, the best and optimal conditions for the organic dye decolorization of MB using TiO_2/Cu_2O nanoparticles as surface adsorbent and photocatalyst, the effective factors on the degradation efficiency including initial dye concertation, the kind and the number of catalysts, pH, temperature, and were then checked and optimized.

Effect of dye concentration on degradation efficiency

The effect of initial dye concentration on both surface adsorption and photodegradation yields was investigated over 4, 8, and 16 mg L^{-1} of MB concentration, respectively. The amount of TiO_2/Cu_2O nanoparticles was fixed at 10 mg and the pH of all dye solutions was adjusted to 6.2. To do the adsorption experiments, initially, the MB solutions with different concentrations were mixed with TiO_2/Cu_2O nanoparticles and stirred under dark conditions for about 1 h. The results are shown in Table 2 and Fig. 5. The surface adsorption yield was calculated 95% and 95.7% for 4.0 mg L^{-1} and 8.0 mg L^{-1} MB respectively, in a very short time (only 1.0 min). However, by increasing the dye concentration to 16.0 mg L^{-1}, the surface adsorption efficiency was decreased to 87.5% (only a slight decrease of about 8.1%). Then to complete the degradation process, three reaction vessels were exposed to ambient light for 1 h and irradiated for another 1 h by a CFL lamp. The results showed a degradation efficiency of 100% for 8.0 mg L^{-1} of MB after 120 min. All the results are shown the high activity of the TiO_2/Cu_2O nanoparticles for degradation of the low, medium, and high concentrations of organic dyes from aqueous media.

Effect of pH

It is well known that the surface charge of photocatalyst and the substrates play a characteristic role in the adsorption/photodegradation yield. When both substrate (here, MB) and photocatalyst carry positive or negative charges, the electrostatic repulses between them lead to the lowest yield of the adsorption/photodegradation process. When the substrate and photocatalyst carry different surface charges, the yield was maximized. The surface charges of substrates and the catalyst can be varied by pH variations around the zpc value (the point of zero charges (pzc). The zpc value is defined as a pH in which the net charge of the solid is equal to zero. The solid reveals positive charges at lower pHs than pHpzc and negative charges at higher pHs than the pHzpc, as reported. Hence, the effect of the pH as one of the most

Table 2 Adsorption/photodegradation results of MB with different concentrations over 4, 8, and 16 ppm by using TiO_2/Cu_2O nanoparticles

Time (min)	A of sample 1 (1.25×10^{-5} M, 4 ppm)	A of sample 2 (2.50×10^{-5} M, 8 ppm)	A of sample 3 (5.00×10^{-5} M, 16 ppm)	Condition
0	0.08	0.116	0.225	–
1	0.004	0.005	0.028	Dark
30	0.001	0.001	0.02	Dark
60	0.001	0.001	0.011	Dark
90	0	0.001	0.01	–
120	0	0	0.01	–
150	0	0	0.01	CFL irradiation
180	0	0	0.01	CFL irradiation

Reaction condition: 15 mL H_2O and 10 mg TiO_2/Cu_2O was sonicated for 30 min then added 15 mL of MB, at pH = 6.2, Compact fluorescent lamp 15 W white

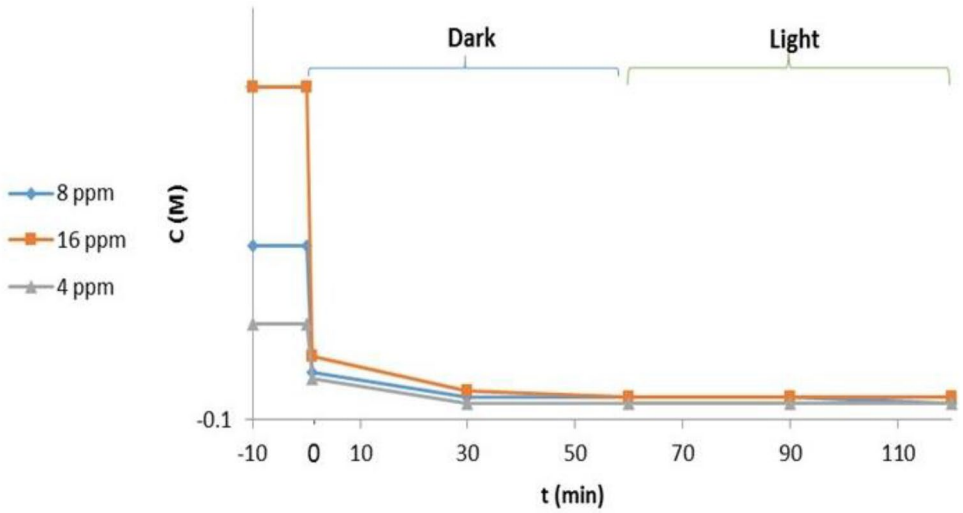

Fig. 5 Effect of initial dye concentration on its photodegradation using TiO_2/Cu_2O nanoparticles

Table 3 Adsorption results of MB on TiO_2/Cu_2O nanoparticles at different pHs

Time (min)	A (pH = 4)	A (pH = 5)	A (pH = 6.2)	A (pH = 8)	Condition
0	0.109	0.102	0.116	0.121	–
1	0.008	0.006	0.005	0.001	Dark
30	0.003	0.002	0.001	0	Dark
60	0.002	0.002	0.001	0	Dark
90[a]	0.001	0.001	0.001	0	–
120[a]	0.001	0.001	0	0	–

Reaction condition:15 mL H_2O and 10 mg Cu_2O/TiO_2 nanoparticles was sonicated 30 min then added 15 mL MB (2.5×10^{-5} M)

[a]Under ambient light

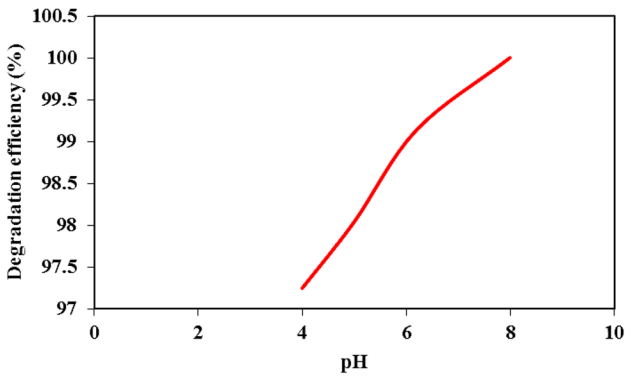

Fig. 6 Effect of pH on degradation efficiency of MB on the surface of TiO_2/Cu_2O nanoparticles

important factors was optimized. The results of adsorption of MB using 10 mg TiO_2/Cu_2O nanoparticles at different pHs are shown in Table 3 and Fig. 6. Based on these results, the adsorption of MB on the surface of TiO_2/Cu_2O nanoparticles was significantly increased and reached 99.2% at pH = 8.0 (it was found to be 92.6% at pH = 4.0). The results are shown in Fig. 6, showing that the photodegradation efficiency was increased from 97.5% at pH = 4.0 to 100.0% at pH = 8.0. This behavior can be explained by the surface charges of MB and TiO_2/Cu_2O nanoparticles at different pHs. The pHzpc of TiO_2 particles is previously reported as

6.8 by Zhao et al. (1993), hence, the surface of photocatalyst is positively charged in acidic solution (pH < 6.8), whereas it is negatively charged in alkaline solution (pH > 6.8). It means that the titania is present as $TiOH_2^+$ in acidic conditions (like pH = 4.0 and 5.0) and TiO^- is its major form presented in the alkaline conditions which can be represented by the following reactions (i.e., Eqs. 1 and 2):

$$Ti - OH + H^+ \Leftrightarrow TiOH_2^+ \ (pH < 6.8), \quad (1)$$

$$Ti - OH + OH^- \Leftrightarrow TiO^- + H_2O \ (pH > 6.8). \quad (2)$$

Moreover, because MB is a cationic dye, the electrostatic interactions between the $TiOH_2^+$ and MB in acidic conditions is occurred at their minimum levels due to the strong repulsion between them, leading to minimizing the adsorption of MB on the surface of the nanoparticles. Besides, due to the short lifetime of ·OH radicals and their low chance for diffusion from the surface of nano-photocatalyst to bulk solution, the photodegradation was also decreased by decreasing the adsorption of the substrate on the surface of the as-prepared nano-photocatalyst. In contrast, at higher pH than 6.8, the adsorption of positively charged MB on the surface of negatively charged nano-photocatalyst occurs at its maximum value, hence, the photodegradation efficiency was also maximized. Hence, pH = 8.0 was selected as optimal pH for MB photodegradation by TiO_2/Cu_2O nanoparticles.

Effect of temperature on MB degradation

The effect of temperature on the photodegradation of MB in the presence of TiO_2/Cu_2O nanoparticles was also checked as one of the most important factors that affect the catalytic activity of nanocatalysts as well as the adsorption capacity of adsorbents. To do this, the adsorption/photodegradation of MB was performed at $T = 50$ °C using 10 mg of TiO_2/Cu_2O nanoparticles as the photocatalyst (Fig. 7). The results showed that after 1.0 min MB was disappeared. The possible reason for this phenomenon is maybe providing more energy for the substrate molecules at high temperatures, hence, the substrate molecules can easily overcome the barrier of activation energy of the surface adsorption/degradation reaction. The results also proved the endothermic nature of the surface adsorption/degradation process of MB on the surface of TiO_2/Cu_2O nanoparticles.

Effect of kinds and amount of catalyst

The effect of nano-photocatalyst on the adsorption/photodegradation process was evaluated as another key parameter on dye decolorization yield. To do this, both adsorption and photodegradation tests were carried out by three different amounts of TiO_2/Cu_2O nanoparticles (i.e., 0.005, 0.01, and 0.02 g). The results are shown in Table 4, showing an adsorption efficiency of 88.7%, 95.7%, and 96.5% for 0.005 g, 0.01 g, and 0.02 g of TiO_2/Cu_2O nanoparticles, respectively, imply that the photoadsorption efficiency was increased by increasing the catalyst amount. Moreover, the photodegradation efficacy was also estimated for 0.005 g, 0.01 g, and 0.02 g of TiO_2/Cu_2O nanoparticles as very high as 99.13%, 100%, and 100%, respectively. Since, by increasing the catalyst amount from 0.01 to 0.02 g, the adsorption/photodegradation yield was not significantly improved, hence, 0.01 g was selected as the optimal catalyst amount based on economic considerations.

In continuing to show the high efficiency of TiO_2/Cu_2O nanoparticles, two kinds of catalysts (Degussa p25 titanium dioxide nanopowder, Cu_2O nanoparticles) were also evaluated by degradation of MB (2.5×10^{-5} M, 8 ppm) in

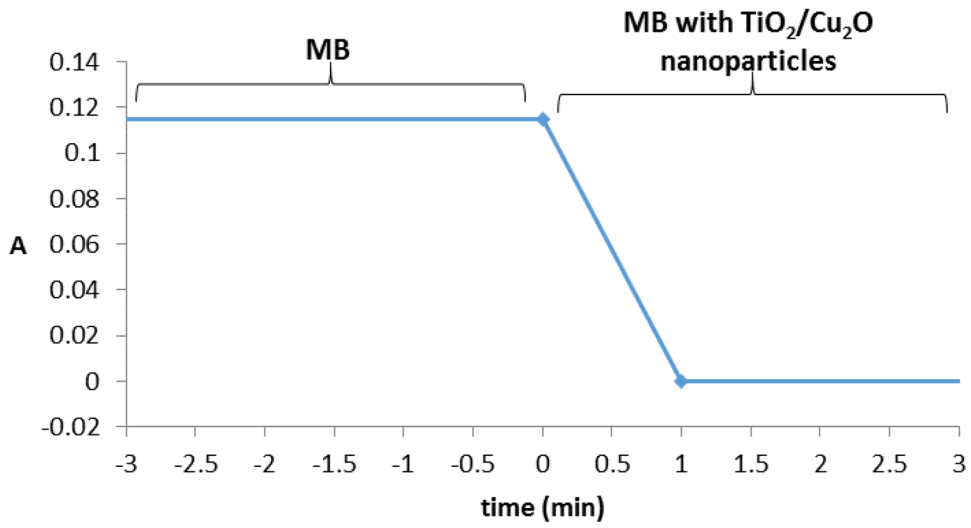

Fig. 7 The degradation efficiency of MB on the surface of TiO_2/Cu_2O nanoparticles at 50 °C

Table 4 Adsorption/photodegradation results for MB degradation using different amounts of TiO_2/Cu_2O nanoparticles

Time (min)	A (0.005 g)	A (0.01 g)	A (0.02 g)	Condition
0	0.116	0.116	0.116	–
1	0.013	0.005	0.004	Dark
30	0.008	0.001	0.001	Dark
60	0.006	0.001	0.001	Dark
90	0.005	0.001	0.001	–
120	0.005	0	0	–
150	0.003	0	0	CFL[b] irradiation
180	0.003	0	0	CFL irradiation
210	0.002	0	0	CFL irradiation
250	0.001	0	0	CFL irradiation
290	0.001	0	0	CFL irradiation

Reaction condition: 15 mL H_2O and $Cu_2O.TiO_2$ nanoparticles was sonicated for 30 min then was added 15 mL of 5.0×10^{-5} M (2.5×10^{-5} M) MB, at pH = 6.2

[b]Compact fluorescent lamp 15 W white

an aqueous solution. Notably, in this study, the amount of Cu_2O and p25 used are those that exist in 10 mg of TiO_2/Cu_2O nanoparticles. The results are shown in Table 5, and Fig. 8. As can be seen from these results, the pure TiO_2 and Cu_2O nanoparticles show lower surface adsorption and photodegradation performances (rate) than the TiO_2/Cu_2O nanoparticles. It is due to the wider surface area and also suitable energy bandgap of the TiO_2/Cu_2O nanoparticles than those of pure TiO_2 and Cu_2O nanoparticles, leading to better $\pi - n$ heterojunction particles in TiO_2/Cu_2O nanoparticles which makes more effective than the pure p25 and Cu_2O nanoparticles.

Degradation mechanism of methylene blue

Based on the results of initial dye concentration on the photodegradation of MB, the MB concertation was dramatically decreased without any photo-irradiation within a very short time (1.0 min) after its incubation with TiO_2/Cu_2O nanoparticles. This is showed that the nanocatalyst can exhibit highly ability dye photodegradation from aqueous media by pre-adsorption of the dye on the surface of TiO_2/Cu_2O nanoparticles. More precisely, during the degradation process, the MB molecules and the oxygen molecules transfer from the solution to the surface of TiO_2/Cu_2O nanoparticles during a very short adsorption

Table 5 Absorption of MB by Cu_2O/TiO_2, Cu_2O and p25

Time (min)	A (Cu_2O/TiO_2)[a]	A (Cu_2O)[b]	A (p25, TiO_2)[c]	Condition
0	0.116	0.116	0.116	–
1	0.005	0.003	0.016	Dark
30	0.001	0.003	0.005	Dark
60	0.001	0.002	0.003	Dark
90	0.001	0.002	0.003	–
120	0	0.002	0.002	–
150	0	0.001	0.002	CFL[d] irradiation

Reaction condition: 15 mL H_2O, [a]10 mg, [b]6 mg, [c]0.6 mg catalyst was sonicated for 30 min then 15 mL MB (2.5×10^{-5} M)was added, pH = 6.2, [d]Compact fluorescent lamp 15 W white.

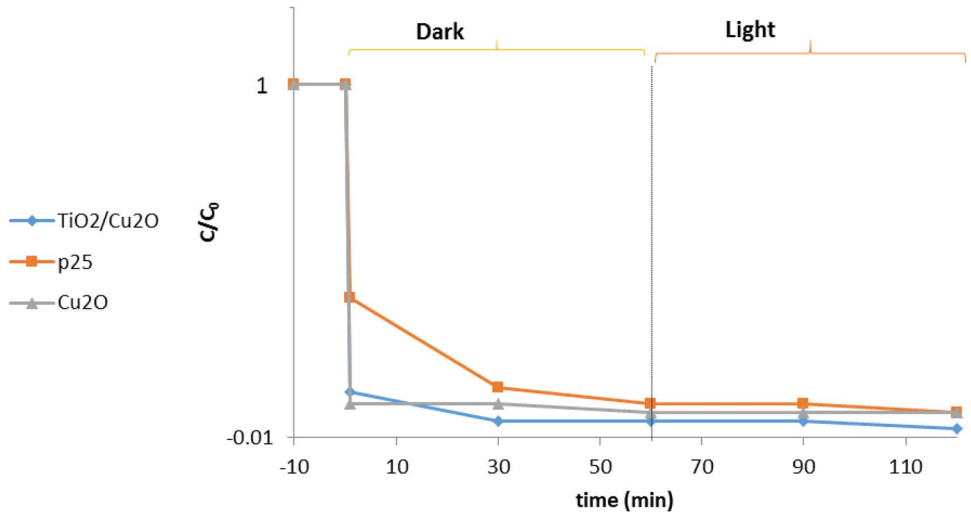

Fig. 8 Surface adsorption and photodegradation yield of MB over TiO_2/Cu_2O nanoparticles, Cu_2O, and p25

time which can enhance the rate and efficiency of the photocatalytic degradation. In contrast, after dark incubation for completing the adsorption process, the Cu_2O was act its role for enhancing the photoactivity of TiO_2 toward dye degradation in the presence of visible light. Considering this fact, the as-prepared TiO_2/Cu_2O nanoparticles can play a characteristic role in the degradation of organic dyes via an adsorption/photodegradation reaction pathway. To prove this hypothesis, The FT-IR spectrum of TiO_2/Cu_2O nanoparticles after incubation with MB under dark was comprised with the FT-IR of MB (Fig. 9). The results showed that the intensity of vibrational peaks related to –C=S and –C=N bands of MB were significantly decreased after incubation with TiO_2/Cu_2O nanoparticles in dark, proving adsorption of MB on the surface of TiO_2/Cu_2O nanoparticles by interaction with –C=S and –C=N groups. Hence, the FT-IR results proved this hypothesis that TiO_2/Cu_2O nanoparticles degraded the MB molecules via an adsorption/photodegradation reaction pathway.

dark conditions.

Based on the above considerations, the primary photocatalytic oxidation mechanism for MB photodegradation on the surface of nanoparticles is proposed which is close to the mechanism reported by Houas et al. (2001).

As found from this mechanism, the hydroxyl radicals were produced on the surface of photo-activated TiO_2/Cu_2O nanoparticles and then the resulting hydroxyl radicals affect the adsorbed MB molecules and degrade them to the corresponding mineral products. The degradation of MB by the resulting hydroxyl radicals can provide the main view on the MB degradation over the photo-activated TiO_2/Cu_2O nanoparticles and the possible intermediates during this process (see SI).

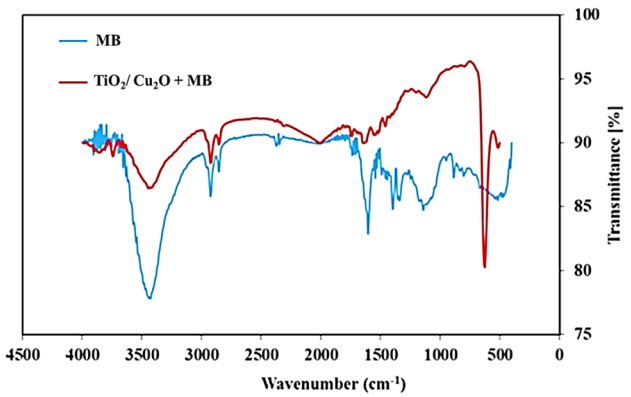

Fig. 9 FT-IR spectrum of MB and TiO_2/Cu_2O after incubation with MB under

Conclusions

In this study, TiO_2/Cu_2O nanoparticles were utilized as cost-effective nano-photocatalysts for high throughput surface adsorption and photodegradation of methylene blue (MB) as a model cationic organic dye. The as-synthesized nanoparticles were characterized by different instrumental characterization methods including ICP, FT-IR, UV–Vis, TEM, and SEM, as well as XRD analyses. Besides, as one of the most properties of a nanomaterial, the surface area and porosity of the as-prepared TiO_2/Cu_2O nano-photocatalysts were also investigated. Regarding the photocatalytic activity evaluations, the as-prepared nano-photocatalysts revealed an adsorption yield as high as 95.7% and a photodegradation efficiency of about 100.0% for methylene blue photodegradation via an adsorption/photodegradation mechanism pathway. It should be noted that in 2018, Pham et al. reported synthesis and characterization of Cu_2O/TiO_2 nanotubes junction for photocatalyst application (Tran et al. 2018). However, they did not optimize the effective factors or kinetic properties of the photodegradation process. The above-mentioned Cu_2O/TiO_2 nanotubes junction showed a photodegradation yield of about 81.7% after a time as high as 150 min while our developed nanoparticles showed about 99% photodegradation yield after time as short as 30.0 min (Tran et al. 2018). Overall, the factors affecting both photoadsorption and photodegradation of MB on the surface of the as-synthesized nanoparticles, for instance, pH, dye initial concertation, amount of TiO_2/Cu_2O nano-photocatalysts, and temperature were optimized. Moreover, to obtain a better view of the photocatalytic performances of TiO_2/Cu_2O nanoparticles, the dye photodegradation was also carried out by both Degussa p25 TiO_2 nanopowder and Cu_2O nanoparticles. The results showed that TiO_2/Cu_2O nanoparticles revealed higher photoadsorption and photodegradation yields toward dye degradation compared to both p25 and pure Cu_2O.

Supplementary Information The online version contains supplementary material available at https://doi.org/10.1007/s13204-022-02474-x.

Acknowledgements Financial support from the research councils of Shiraz University is gratefully acknowledged.

Author contributions The manuscript was written through the contributions of all authors. All authors have approved the final version of the manuscript.

Declarations

Conflict of interest There are no conflicts of interest to declare.

References

Aguirre ME, Zhou R, Eugene AJ, Guzman MI, Grela MA (2017) Cu_2O/TiO_2 heterostructures for CO_2 reduction through a direct Z-scheme: Protecting Cu_2O from photocorrosion. Appl Catal B 217:485–493

Ahmad A, Rafatullah M, Sulaiman O, Ibrahim MH, Hashim R (2009) Scavenging behaviour of meranti sawdust in the removal of methylene blue from aqueous solution. J Hazard Mater 170(1):357–365

Ahmad T, Rafatullah M, Ghazali A, Sulaiman O, Hashim R (2011) Oil palm biomass–Based adsorbents for the removal of water pollutants—a review. J Environ Sci Health Part C 29:177–222

Ahmad T, Danish M, Rafatullah M, Ghazali A, Sulaiman O, Hashim R, Ibrahim MNM (2012) The use of date palm as a potential adsorbent for wastewater treatment: a review. Environ Sci Pollut Res 19(4):1464–1484

Ahmed MA, Abou-Gamra ZM, Salem AM (2017) Photocatalytic degradation of methylene blue dye over novel spherical mesoporous Cr_2O_3/TiO_2 nanoparticles prepared by sol-gel using octadecylamine template. J Environ Chem Eng 5(5):4251–4261

Akpan UG, Hameed BH (2009) Parameters affecting the photocatalytic degradation of dyes using TiO_2-based photocatalysts: a review. J Hazard Mater 170(2–3):520–529

Aksu Z (2005) Application of biosorption for the removal of organic pollutants: a review. Process Biochem 40(3–4):997–1026

Almeida CA, Debacher NA, Downs AJ, Cottet L, Mello CA (2009) Removal of methylene blue from colored effluents by adsorption on montmorillonite clay. J Colloïd Interface Sci 332(1):46–53

Aravind M, Ahmad A, Ahmad I, Amalanathan M, Naseem K, Mary SM, Parvathiraja C, Hussain S, Algarni TS, Pervaiz M, Zuber M (2021) Critical green routing synthesis of silver NPs using jasmine flower extract for biological activities and photocatalytical degradation of methylene blue. J Environ Chem Eng 9(1):104877

Cao R, Yang H, Deng X, Zhang S, Xu X (2017) In-situ synthesis of amorphous silver silicate/carbonate composites for selective visible-light photocatalytic decomposition. Sci Rep 7(1):1–2

Chen D, Cheng Y, Zhou N, Chen P, Wang Y, Li K, Huo S, Cheng P, Peng P, Zhang R, Wang L (2020) Photocatalytic degradation of organic pollutants using TiO_2-based photocatalysts: a review. J Clean Prod 268:121725

de Jongh PE, Vanmaekelbergh D, Kelly JJ (1999) Cu_2O: a catalyst for the photochemical decomposition of water? Chem Commun 12:1069–1070

Ding F, Xie Y, Peng W, Peng YK (2016) Measuring the bioactivity and molecular conformation of typically globular proteins with phenothiazine-derived methylene blue in solid and in solution: A comparative study using photochemistry and computational chemistry. J Photochem Photobiol B 158:69–80

Eltaweil AS, Elgarhy GS, El-Subruiti GM, Omer AM (2020) Carboxymethyl cellulose/carboxylated graphene oxide composite microbeads for efficient adsorption of cationic methylene blue dye. Int J Biol Macromol 154:307–318

Fagan R, McCormack DE, Dionysiou DD, Pillai SC (2016) A review of solar and visible light active TiO_2 photocatalysis for treating bacteria, cyanotoxins and contaminants of emerging concern. Mater Sci Semicond Process 1(42):2–14

Forgacs E, Cserhati T, Oros G (2004) Removal of synthetic dyes from wastewaters: a review. Environ Int 30(7):953–971

Ghafoor S, Ata S, Mahmood N, Arshad SN (2017) Photosensitization of TiO_2 nanofibers by Ag_2S with the synergistic effect of excess surface Ti^{3+} states for enhanced photocatalytic activity under simulated sunlight. Sci Rep 7(1):1

Gupta VK (2009) Application of low-cost adsorbents for dye removal—a review. J Environ Manage 90(8):2313–2342

Han C, Li Z, Shen J (2009) Photocatalytic degradation of dodecylbenzenesulfonate over TiO_2–Cu_2O under visible irradiation. J Hazard Mater 168(1):215–219

He X, Wang A, Wu P, Tang S, Zhang Y, Li L, Ding P (2020) Photocatalytic degradation of microcystin-LR by modified TiO_2 photocatalysis: a review. Sci Total Environ 743:140694

Hong Y, Tian C, Jiang B, Wu A, Zhang Q, Tian G, Fu H (2013) Facile synthesis of sheet-like ZnO assembly composed of small ZnO particles for highly efficient photocatalysis. J Mater Chem A 1(18):5700–5708

Hosseini-Sarvari M, Dehghani A (2020) Visible-light-driven photochemical activity of ternary $Ag/AgBr/TiO_2$ nanotubes for oxidation C (sp^3)–H and C (sp^2)–H bonds. New J Chem 44(39):16776–16785

Hosseini-Sarvari M, Hosseinpour Z (2019) Synthesis of Ag nanoparticles decorated on TiO_2 nanotubes for surface adsorption and photo-decomposition of methylene blue under dark and visible light irradiation. Res Chem Intermed 45(4):1829–1840

Hosseini-Sarvari M, Jafari F (2020) TiO_2/Cu_2O nanoparticle-catalyzed direct C (sp)–P bond formation via aerobic oxidative coupling in air and visible light. Dalton Trans 49:3001–3006

Hosseini-Sarvari M, Koohgard M, Firoozi S, Mohajeri A, Tavakolian H (2018a) Alizarin red S–TiO_2-catalyzed cascade C (sp^3)–H to C (sp^2)–H bond formation/cyclization reactions toward tetrahydroquinoline derivatives under visible light irradiation. New J Chem 42(9):6880–6888

Hosseini-Sarvari M, Jafari F, Mohajeri A, Hassani N (2018b) Cu_2O/TiO_2 nanoparticles as visible light photocatalysts concerning C (sp^2)–P bond formation. Catal Sci Technol 8(16):4044–4051

Houas A, Lachheb H, Ksibi M, Elaloui E, Guillard C, Herrmann JM (2001) Photocatalytic degradation pathway of methylene blue in water. Appl Catal B 31(2):145–157

Joshi KM, Shrivastava VS (2011) Degradation of alizarine red-S (A textiles dye) by photocatalysis using ZnO and TiO_2 as photocatalyst. Int J Environ Sci 2(1):8–21

Khasawneh OFS, Palaniandy P (2021) Removal of organic pollutants from water by Fe_2O_3/TiO_2 based photocatalytic degradation: a review. Environ Technol Innov 21:101230

Kuriechen SK, Murugesan S, Raj SP, Maruthamuthu P (2011) Visible light assisted photocatalytic mineralization of Reactive Red 180 using colloidal TiO_2 and oxone. Chem Eng J 174(2–3):530–538

Lee QY, Li H (2021) Photocatalytic degradation of plastic waste: a mini review. Micromachines 12(8):907

Li Y, Wang B, Liu S, Duan X, Hu Z (2015) Synthesis and characterization of Cu_2O/TiO_2 photocatalysts for H_2 evolution from aqueous solution with different scavengers. Appl Surf Sci 324:736–744

Li G, Huang J, Chen J, Deng Z, Huang Q, Liu Z, Guo W, Cao R (2019) Highly active photocatalyst of Cu_2O/TiO_2 octahedron for hydrogen generation. ACS Omega 4(2):3392–3397

Li Y, Zhang P, Wan D, Xue C, Zhao J, Shao G (2020a) Direct evidence of 2D/1D heterojunction enhancement on photocatalytic activity through assembling MoS2 nanosheets onto super-long TiO_2 nanofibers. Appl Surf Sci 504:144361

Li R, Li T, Zhou Q (2020b) Impact of titanium dioxide (TiO_2) modification on its application to pollution treatment—a review. Catalysts 10(7):804

Lin Y, Zhang F, Pan D, Li H, Lu Y (2012) Sunlight-driven photodegradation of organic pollutants catalyzed by $TiO_2/(ZnS)_x(CuInS_2)_{1-x}$ nanocomposites. J Mater Chem 22(18):8759–8763

Linsebigler AL, Lu G, Yates JT Jr (1995) Photocatalysis on TiO_2 surfaces: principles, mechanisms, and selected results. Chem Rev 95(3):735–758

Liu L, Yang W, Li Q, Gao S, Shang JK (2014) Synthesis of Cu_2O nanospheres decorated with TiO_2 nanoislands, their enhanced photoactivity and stability under visible light illumination, and

their post-illumination catalytic memory. ACS Appl Mater Interfaces 6(8):5629–5639
Lucas MS, Peres JA (2007) Degradation of reactive Black 5 by Fenton/UV-C and ferrioxalate/H_2O_2/solar light processes. Dyes Pigm 74(3):622–629
Mashkoor F, Nasar A (2020) Magsorbents: Potential candidates in wastewater treatment technology—a review on the removal of methylene blue dye. J Magnet Magnet Mater 500:166408
Messih MA, Ahmed MA, Soltan A, Anis SS (2017) Facile approach for homogeneous dispersion of metallic silver nanoparticles on the surface of mesoporous titania for photocatalytic degradation of methylene blue and indigo carmine dyes. J Photochem Photobiol A 335:40–51
Mohabansi NP, Patil VB, Yenkie N (2011) A comparative study on photo degradation of methylene blue dye effluent by advanced oxidation process by using TiO_2/ZnO photo catalyst. Rasayan J Chem 4(4):814–819
Muruganandham M, Swaminathan M (2004) Solar photocatalytic degradation of a reactive azo dye in TiO_2-suspension. Sol Energy Mater Sol Cells 81(4):439–457
Muscetta M, Andreozzi R, Clarizia L, Di Somma I, Marotta R (2020) Hydrogen production through photoreforming processes over Cu_2O/TiO_2 composite materials: a mini-review. Int J Hydrog Energy 45(53):28531–28552. https://doi.org/10.1016/j.ijhydene.2020.07.225
Onwuka KE, Achilike K, Eze KS (2021) Montmorillonite clay enhanced TiO_2 nanoparticle for photocatalytic degradation of organic pollutants: mini review. Int J Pharma Sci 1(1):33–38
Özer A, Dursun G (2007) Removal of methylene blue from aqueous solution by dehydrated wheat bran carbon. J Hazard Mater 146(1–2):262–269
Ponnusami V, Vikram S, Srivastava SN (2008) Guava (*Psidium guajava*) leaf powder: novel adsorbent for removal of methylene blue from aqueous solutions. J Hazard Mater 152(1):276–286
Rahimian R, Zarinabadi S (2020) A review of studies on the removal of methylene blue dye from industrial wastewater using activated carbon adsorbents made from almond bark. Progress Chem Biochem Res 3(3):251–268
Saeed A, Iqbal M, Zafar SI (2009) Immobilization of Trichoderma viride for enhanced methylene blue biosorption: batch and column studies. J Hazard Mater 168(1):406–415
Santoso E, Ediati R, Kusumawati Y, Bahruji H, Sulistiono DO, Prasetyoko D (2020) Review on recent advances of carbon based adsorbent for methylene blue removal from waste water. Mater Today Chem 16:100233
Şengil İA, Özacar M (2009) The decolorization of CI Reactive Black 5 in aqueous solution by electrocoagulation using sacrificial iron electrodes. J Hazard Mater 161(2–3):1369–1376
Slokar YM, Le Marechal AM (1998) Methods of decoloration of textile wastewaters. Dyes Pigm 37(4):335–356
Somasiri W, Li XF, Ruan WQ, Jian C (2008) Evaluation of the efficacy of upflow anaerobic sludge blanket reactor in removal of colour and reduction of COD in real textile wastewater. Biores Technol 99(9):3692–3699
Tavakolian M, Keshavarz K, Hosseini-Sarvari M (2021) Cu_2O/TiO_2 as a sustainable and recyclable photocatalyst for gram-scale synthesis of phenols in water. Mol Catal 514:111810
Tran HH, Cao MT, Nguyen TK, Kim YS (2018) Photoreduction route for Cu_2O/TiO_2 nanotubes junction for enhanced photocatalytic activity. RSC Adv 8(22):12420–12427
Wang Q, Yang Z (2016) Industrial water pollution, water environment treatment, and health risks in China. Environ Pollut 218:358–365
Wang M, Sun L, Lin Z, Cai J, Xie K, Lin C (2013) p–n Heterojunction photoelectrodes composed of Cu_2O-loaded TiO_2 nanotube arrays with enhanced photoelectrochemical and photoelectrocatalytic activities. Energy Environ Sci 6(4):1211–1220
Wei Z, Liu J, Shangguan W (2020) A review on photocatalysis in antibiotic wastewater: pollutant degradation and hydrogen production. Chin J Catal 41(10):1440–1450
Xiong Z, Dou H, Pan J, Ma J, Xu C, Zhao XS (2010) Synthesis of mesoporous anatase TiO_2 with a combined template method and photocatalysis. CrystEngComm 12(11):3455–3457
Xu J, Li S, Wang F, Yang Z, Liu H (2019) Efficient and enhanced adsorption of methylene blue on triethanolamine-modified graphene oxide. J Chem Eng Data 64(4):1816–1825
Yang J, Qiu K (2010) Preparation of activated carbons from walnut shells via vacuum chemical activation and their application for methylene blue removal. Chem Eng J 165(1):209–217
Yang L, Luo S, Li Y, Xiao Y, Kang Q, Cai Q (2010) High efficient photocatalytic degradation of p-nitrophenol on a unique Cu_2O/TiO_2 pn heterojunction network catalyst. Environ Sci Technol 44(19):7641–7646
Zaied M, Bellakhal N (2009) Electrocoagulation treatment of black liquor from paper industry. J Hazard Mater 163(2–3):995–1000
Zhang S, Peng B, Yang S, Fang Y, Peng F (2013) Non-noble metal copper nanoparticles-decorated TiO_2 nanotube arrays with plasmon-enhanced photocatalytic hydrogen evolution under visible light. Int J Hydrogen Energy 38(32):13866–13871
Zhao J, Hidaka H, Takamura A, Pelizzetti E, Serpone N (1993) Photodegradation of surfactants. 11. zeta.-Potential measurements in the photocatalytic oxidation of surfactants in aqueous titania dispersions. Langmuir 9(7):1646–1650
Zheng Z, Huang B, Wang Z, Guo M, Qin X, Zhang X, Wang P, Dai Y (2009) Crystal faces of Cu_2O and their stabilities in photocatalytic reactions. J Phys Chem C 113(32):14448–14453
Zou JP, Wu DD, Luo J, Xing QJ, Luo XB, Dong WH, Luo SL, Du HM, Suib SL (2016) A strategy for one-pot conversion of organic pollutants into useful hydrocarbons through coupling photodegradation of MB with photoreduction of CO_2. ACS Catal 6(10):6861–6867
Dharma J, Pisal A, Shelton CT (2009) Simple method of measuring the band gap energy value of TiO_2 in the powder form using a UV/Vis/NIR spectrometer. Application Note Shelton: PerkinElmer, pp 1–4